

# UV–visible absorption spectra of alkyl-, vinyl-, aryl- and thiylperoxyl radicals and some related radicals in aqueous solution: a quantum-chemical study

Sergej Naumov<sup>1\*</sup> and Clemens von Sonntag<sup>1,2</sup>

<sup>1</sup>Leibniz Institut für Oberflächenmodifizierung (IOM), Permoserstrasse 15, D-04303 Leipzig, Germany

<sup>2</sup>Max-Planck-Institut für Bioorganische Chemie, Stiftstrasse 34–36, P.O. Box 101365, D-45413 Mülheim an der Ruhr, Germany

Received 28 October 2004; revised 22 December 2004; accepted 30 December 2004



**ABSTRACT:** Alkylperoxyl and alkoxy radicals absorb only in the UV region, whereas vinylperoxyl, phenylperoxyl, alkylthiylperoxyl and benzyloxy radicals have strong absorptions in the visible region. Using the UTD/B3LYP/6–31G+(d,p) method, we calculated the long-wavelength absorption maxima of these and related radicals *in vacuo* and in aqueous solution. The latter were accounted for with a continuum model (SCRF = PCM). The vinylperoxyl radical long-wavelength absorption band is due to a  $-2\beta[\pi] \rightarrow 0\beta[n(O)_z]$  transition. The  $n(O)_y$  orbital lies above the  $\pi$  orbital, but since it is orthogonal to the  $n(O)_z$  orbital, the oscillator strength of the  $-1\beta[n(O)_y] \rightarrow 0\beta[n(O)_z]$  transition is close to zero. Upon chlorine substitution, the first absorption band is red shifted. The  $\pi$  orbital is now raised above the  $n(O)_y$  orbital, and the transition is denoted  $-1\beta[\pi] \rightarrow 0\beta[n(O)_z]$ . The absorption of the phenylperoxyl radical in the visible region is accounted for by two nearby transitions of the same type, i.e.  $-2\beta[\pi] \rightarrow 0\beta[n(O)_z]$  and  $-1\beta[\pi] \rightarrow 0\beta[n(O)_z]$ . Owing to the charge-transfer character of these transitions, there is a marked red shift on going from the gas phase to aqueous solutions. The benzyloxy and phenoxy methyl radicals are related to the phenylperoxyl radicals in so far as one of the peroxyl oxygens is replaced by a methylene group. The benzyloxy radical also absorbs in the visible region and the transition is of the  $-2\beta[\pi] \rightarrow 0\beta[n(O)_z]$  plus  $-1\beta[\pi] \rightarrow 0\beta[n(O)_z]$  type, i.e. it is closely related to that of the phenylperoxyl radical. The phenoxy methyl radical only absorbs in the UV region ( $\lambda_{\max} = 320$  nm; spectrum obtained by pulse radiolysis) and this absorption band is due to  $0\alpha[\pi] \rightarrow +2\alpha[\pi^*]$  plus  $-1\beta[\pi] \rightarrow 0\beta[\pi]$  transitions. The absorption in the visible region of the alkylthiylperoxyl radical is a  $-1\beta[S_z] \rightarrow 0\beta[n(O)_z]$  transition. Alkylthiyl and some other sulfur- and carbon-centered radicals react reversibly with  $O_2$ . The energetics of these reactions were addressed by DFT quantum-chemical calculations. Copyright © 2005 John Wiley & Sons, Ltd.

Supplementary electronic material for this paper is available in Wiley InterScience at <http://www.interscience.wiley.com/jpages/0894-3230/suppmat/>

**KEYWORDS:** UV–visible absorption spectra; peroxyl radicals; DFT calculations

## INTRODUCTION

Many free radicals have strong absorptions in the UV–visible (Vis) region. Often, their absorption maxima are red shifted with respect to the compounds from which the radicals are generated, and in flash photolysis and pulse radiolysis one commonly makes use of this to characterize an intermediate and to follow its reactions.

Peroxy radicals,  $ROO\cdot$ , have usually only uncharacteristic and weak absorptions in the UV region. Although this property can be used, and has been used, with advantage to measure the rate of reaction of  $O_2$  with a given radical, the subsequent reactions of the peroxy radicals are often difficult to follow, and one may have to use other detection techniques, e.g. conductometry, to monitor their unimolecular decay by  $HO_2$  ( $H^+ + O_2^-$ ) release.<sup>1,2</sup>

\*Correspondence to: S. Naumov, Leibniz Institut für Oberflächenmodifizierung (IOM), Permoserstrasse 15, D-04303 Leipzig, Germany. E-mail: [sergej.naumov@iom-leipzig.de](mailto:sergej.naumov@iom-leipzig.de)

It was very surprising when for some peroxy radicals strong absorptions in the visible range were observed. The exception from the rule (only weak absorptions in the UV region) are the vinyl-,<sup>3</sup> aryl-<sup>4–8</sup> and thiylperoxyl radicals,<sup>9–11</sup> but also for the benzyloxy radical,<sup>12,13</sup> another oxygen-centered non-conjugated radical, a long-wavelength absorption has been reported. Strong mesomerism is usually quoted as an explanation for strong red shifts, but this classical approach must fail here.

About 10 years ago, we attempted to calculate with quantum-chemical methods the absorption spectra of such and related radicals. For most of them, agreement between experiment and theory was not fully satisfactory (see also Refs. 14 and 15). This showed that the level of theory available at the time was insufficient, especially for the prediction of the position of the absorption maximum of an as yet not well-characterized free-radical intermediate. In the meantime, the quantum-chemical tools have improved considerably, and we decided to resume the project.

In this work, quantum-chemical calculations of the UV-Vis absorption spectra and oscillator strengths of various kinds of peroxy radicals and structurally related radicals were calculated *in vacuo* and in aqueous solution (to match the experimental conditions) at the UTD/B3LYP/6-31G+(d,p) level of theory. In general, there is now fairly good agreement between theory and experiment, but some deviations still persist. The large number of radicals that are reported here illustrates very clearly to what extent experiment and theory may match. This is of importance in cases where quantum-chemical calculations are used to distinguish between various conceivable intermediates that could be formed in a free-radical reaction.

## EXPERIMENTAL

### Quantum chemical calculations

The calculations were carried out using the Gaussian 03 package.<sup>16</sup> For the systems under study, geometries were optimized applying the density functional theory (DFT) approach with B3LYP hybrid functionals.<sup>17-19</sup> Stationary points were characterized by frequency calculations. Molecular orbitals (MOs) were visualized in graphical form with the help of the GaussView 2.1 program.<sup>20</sup> For geometry optimisations, the standard 6-31+G(d,p) basis sets was used. To investigate the influence of a solvent on the molecular structure of the peroxy radicals, geometry optimizations were carried out using two self-consistent reaction field (SCRF) models: the polarized continuum CPCM<sup>21,22</sup> and the PCM<sup>23,24</sup> models.

The UV-Vis absorption spectra were calculated for the gas phase and in an aqueous environment with the Unrestricted Time Dependent (UTD DFT)<sup>25</sup> B3LYP method. To explore the most reliable method for the calculation of electronic transitions, a large variety of different basis sets, namely 6-31G(d), 6-31G(d,p), 6-311G(d,p), 6-31+G(d,p), 6-31++G(d,p), 6-311+G(d,p) and the highly extended 6-311++G(3df,2p) basis sets, were compared at a molecular geometry optimized in water with the 6-31+G(d,p) basis set. The dependence of the calculated excitation energies on the basis set used and the experimental values are presented for two peroxy radicals,  $\text{CH}_2=\text{CHOO}^\bullet$  (SCRF = PCM) and  $\text{CH}_3\text{SOO}^\bullet$  (SCRF = CPCM), in Fig. 1(a).

The comparison shows a considerable improvement in the agreement with the experiment, when diffuse functions on heavy atoms are included, but basis sets larger than 6-31+G(d,p) lead to only minor improvements. Therefore, the 6-31+G(d,p) basis set was used for both geometry optimizations and calculations of electronic transitions. The numbering of the MOs that are responsible for the long-wavelength transition are shown schematically in Fig. 1(b).

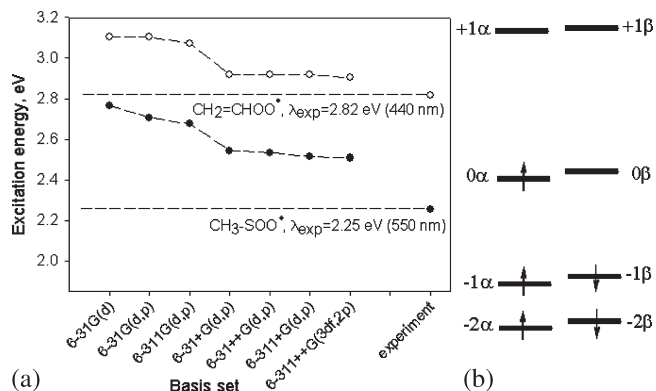


**Figure 1.** (a) Basis set dependence of calculated excitation energies in water of  $\text{CH}_2=\text{CHOO}^\bullet$  (B3LYP//SCRF = PCM) and  $\text{CH}_3\text{SOO}^\bullet$  (B3LYP//SCRF = CPCM) at a geometry optimized in water with B3LYP/6-31+G(d,p); experimental values are given for comparison. (b) Definition of the MOs that are relevant for the long-wavelength transitions of these radicals

To test polarity effects of solvents on the geometric parameters and electronic transition spectra of the peroxy radicals, calculations were made [UTD/B3LYP/6-31G+(d,p)/SCRF = PCM] for the most stable conformer of  $\text{CHCl}=\text{CHOO}^\bullet$  (**3E**, see Table 2) at an optimized molecular structure in the given solvent and for the phenylperoxy radical [UTD/B3LYP/6-31G+(d,p)/SCRF = CPCM] at a fixed gas-phase molecular geometry. Whereas solvents influence the molecular structure only marginally ( $\leq 0.0002 \text{ nm}$  for bond lengths in the case of  $\text{CHCl}=\text{CHOO}^\bullet$ ), they affect considerably the energy of the electronic transitions, and taking their dielectric continuum into account is essential for improving the calculated values with respect to the experimental ones (Table 1).

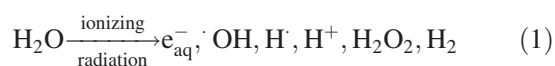
### Pulse radiolysis studies

The UV spectrum of the phenoxymethyl radical, which was included in our calculations for comparison with the oxygen-centered radicals that we are mainly concerned with here, was not available in the literature. We therefore produced this radical in aqueous solution with the help of the pulse radiolysis technique. For the experiment shown below, we used the electron accelerator (Elektronika, Thorium, Moscow) at the IOM. It delivers 10 MeV electron pulses of 7 ns duration. The dose, 46 Gy per pulse, was determined with the help of the thiocyanate dosimeter taking  $G \times \varepsilon = 5.2 \times 10^{-4} \text{ m}^2 \text{ J}^{-1}$  for the formation of  $(\text{SCN})_2^{\bullet-}$  in  $\text{N}_2\text{O}$ -saturated solution.<sup>26</sup>

In the radiolysis of water,  $\text{OH}^\bullet$ , hydrated electrons ( $e_{\text{aq}}^-$ ) and  $\text{H}^\bullet$  are generated [reaction (1)]. The radiation-chemical yields ( $G$  values) of the primary radicals are  $G(\text{OH})G(e_{\text{aq}}^-) \approx 2.9 \times 10^{-7} \text{ mol J}^{-1}$  and  $G(\text{H}) = 0.6 \times 10^{-7} \text{ mol J}^{-1}$ .

**Table 1.** Calculated absorption maxima (nm) of the long-wavelength transitions of  $\text{CHCl=CHOO}^\cdot$  [UTD/B3LYP/6-31+G(d,p)/SCRF = PCM at a molecular structure optimized for the given solvent] and of  $\text{PhOO}^\cdot$  [UTD/B3LYP/6-31+G(d,p)/SCRF = CPCM at gas-phase molecular structure] as a function of the dielectric constant of the environment (oscillator strengths in parentheses)

Solvent	$\text{CHCl=CHOO}^\cdot$ $-1\beta[\pi] \rightarrow 0\beta[\text{n}(\text{O})_z]$	$\text{PhOO}^\cdot$	
		$-2\beta[\pi] \rightarrow 0\beta[\text{n}(\text{O})_z]$	$-1\beta[\pi] \rightarrow 0\beta[\text{n}(\text{O})_z]$
Vacuum, $\epsilon = 1$	426 (0.092)	409 (0.022)	448 (0.062)
Argon, $\epsilon = 1.43$	438 (0.112)	428 (0.031)	466 (0.072)
Heptane, $\epsilon = 1.92$	447 (0.127)	439 (0.034)	479 (0.083)
Cyclohexane, $\epsilon = 2.02$	449 (0.130)	441 (0.085)	481 (0.035)
Tetrahydrofuran, $\epsilon = 7.58$	461 (0.140)	471 (0.054)	503 (0.073)
Dichloromethane, $\epsilon = 8.93$	462 (0.142)	473 (0.055)	506 (0.074)
Acetone, $\epsilon = 20.70$	463 (0.141)	479 (0.063)	510 (0.063)
Methanol, $\epsilon = 32.63$	463 (0.140)	480 (0.066)	511 (0.059)
Acetonitrile, $\epsilon = 36.64$	464 (0.141)	480 (0.066)	512 (0.060)
Nitromethane, $\epsilon = 38.2$	465 (0.143)	481 (0.065)	513 (0.063)
Water, $\epsilon = 78.39$	464 (0.141)	482 (0.068)	513 (0.058)
Water, $\epsilon = 78.39$	480 (experiment)	490 (experiment)	490 (experiment)



The solvated electron can be converted with  $\text{N}_2\text{O}$  into further  $\cdot\text{OH}$ :



At high pH,  $\text{H}^\cdot$  is converted into  $\text{e}_{\text{aq}}^-$  [reaction (3)], and  $\cdot\text{OH}$  is in equilibrium with  $\text{O}^{\cdot-}$  [ $\text{p}K_{\text{a}}(\cdot\text{OH}) = 11.8$ ].



Whereas with anisole  $\cdot\text{OH}$  reacts by an addition to the ring,  $\text{O}^{\cdot-}$  undergoes mainly H-abstraction:



Hence, in  $\text{N}_2\text{O}$ -saturated solution at pH 14, the spectrum that is obtained after the pulse is that of the phenoxy-methyl radical (Fig. 2). Its absorption maximum is at

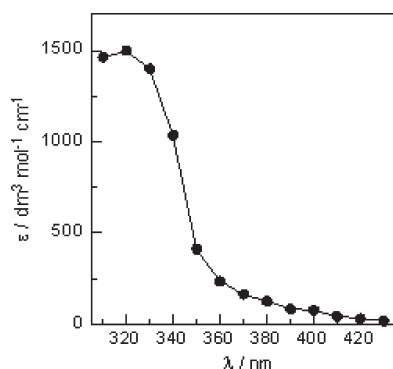


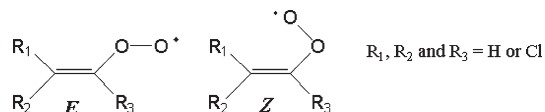
**Figure 2.** Pulse radiolysis of  $\text{N}_2\text{O}$ -saturated aqueous solutions of anisole (saturated) at pH 14. Spectrum of the phenoxy-methyl radical **13**

320 nm with a molar absorption coefficient of  $1500 \text{ dm}^3 \text{ mol}^{-1} \text{ cm}^{-1}$ .

## RESULTS AND DISCUSSION

The experimental spectra of the vinylperoxyl radicals were mainly obtained in water by pulse radiolysis, whereas those of the oxyl radicals were generated by laser flash photolysis in an organic solvent. For this reason, the calculations of the spectra have to take solvent effects into account. After the geometry of the radicals had been calculated *in vacuo*, solvent effects were approximated by a continuum model that mimics the dielectric constant of the solvent but, for water, still neglects potential effects due to hydrogen bonding. With this approach and for most spectra that we deal with here, marked red shifts are observed on going from vacuum to water solutions (see Tables 1–4).

For the vinylperoxyl radicals, two isomers with *E* and *Z* conformations may be written. The *E* conformer is generally more stable (second column in Tables 2 and 3), but owing to small activation energies of C–O rotation often all intermediate conformations may be populated and contribute to the observed absorption.



The one but last column in Tables 2–4 shows the maximum of the absorption spectrum as obtained by pulse radiolysis in aqueous solution. The agreement between the experimental and calculated data is usually acceptable, and the trends induced by substitution are well reflected. The transition, given in the last column, is defined as shown in Fig. 1(b) and is discussed in more detail below.

**Table 2.** Calculation of the absorption maxima (oscillator strengths in parentheses) of the long-wavelength band of some peroxy radicals using the UTD/B3LYP/6-31G+(d,p) method *in vacuo* and in water (SCRF = PCM)<sup>a</sup>

Radical	Conformer	$\Delta E$ , $E$ vs $Z$ (kJ mol <sup>-1</sup> )	$\lambda_{\text{calc}}$ (nm)		$\lambda_{\text{exp}}$ (nm)	Transition
			Vacuum	Water		
	<b>1E</b>	5.9 (6.1)	389 (0.069)	425 (0.104)	440 (Ref. 3)	$-2\beta[\pi] \rightarrow 0\beta[n(\text{O})_z]$
	<b>1Z</b>		438 (0.040)	482 (0.056)		
	<b>2E</b>	0.4 (3.9)	432 (0.053)	467 (0.078)	480 (Ref. 3)	$-1\beta[\pi] \rightarrow 0\beta[n(\text{O})_z]$
	<b>2Z</b>		514 (0.023)	562 (0.032)		
	<b>3E</b>	4.0 (1.1)	426 (0.092)	464 (0.141)	480 (Ref. 3)	$-1\beta[\pi] \rightarrow 0\beta[n(\text{O})_z]$
	<b>3Z</b>		489 (0.062)	534 (0.089)		
	<b>4E</b>	19.0 (1.1)	453 (0.089)	495 (0.134)	540 (Ref. 3)	$-1\beta[\pi] \rightarrow 0\beta[n(\text{O})_z]$
	<b>4Z</b>		472 (0.061)	511 (0.089)		
	<b>5E</b>	0.3 (5.1)	456 (0.077)	493 (0.117)	540 (Ref. 3)	$-1\beta[\pi] \rightarrow 0\beta[n(\text{O})_z]$
	<b>5Z</b>		562 (0.042)	610 (0.059)		
	<b>6E</b>	14.6 (17.1)	482 (0.061)	528 (0.088)	540 (Ref. 3)	$-1\beta[\pi] \rightarrow 0\beta[n(\text{O})_z]$
	<b>6Z</b>		539 (0.038)	581 (0.044)		
	<b>7E</b>	19.7 (21.7)	489 (0.071)	533 (0.106)	580 (Ref. 3)	$-1\beta[\pi] \rightarrow 0\beta[n(\text{O})_z]$
	<b>7Z</b>			530 <sup>b</sup> 538 <sup>c</sup>		
	<b>8</b>		372 (0.004)	412 (0.015)	430 (Ref. 27)	$-2\beta[\pi] \rightarrow 0\beta[n(\text{O})_z]$

<sup>a</sup> Transitions as defined in the text. The energy differences ( $\Delta E$ ) for the  $E$  and  $Z$  conformers *in vacuo* and in water (in parentheses).<sup>b</sup> 6-311G+(d,p) basis set.<sup>c</sup> SCRF = CPCM (COSMO).

## Nature of the long-wavelength transitions

Figure 3(a) shows the orbitals responsible for the long-wavelength transition in the vinylperoxy radical **1**.

The transition occurs from the highest occupied  $\pi$  orbital to the  $\beta(\text{O})_z$  orbital of the peroxy oxygens,  $-2\beta[\pi] \rightarrow 0\beta[n(\text{O})_z]$ . This is a kind of intramolecular charge transfer, and for this reason it is not surprising that the solvent polarity influences markedly the energy of this transition. The  $n(\text{O})_y$  orbital is orthogonal to the  $n(\text{O})_z$  orbital and the oscillator strength of this transition is near zero.

Upon chlorine substitution [Fig. 3(b)] the positions of the  $n(\text{O})_y$  and  $n(\text{O})_z$  orbitals remain the same, but the  $\pi$  orbital is raised. As a consequence, the absorption maxima of **2–7** are red shifted. As an example, the sequence of the relevant orbitals is shown for the trichlorovinylperoxy radical **7** in Fig. 3(b).

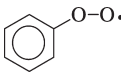
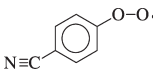
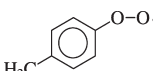
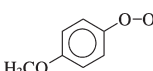
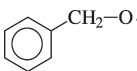
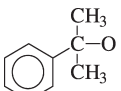
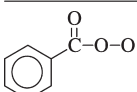
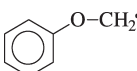
Interestingly, interlacing a  $\text{C}=\text{O}$  group between the vinyl group and the peroxy function as in **8** also leads to a peroxy radical that absorbs in the visible region. In fact, it is the same type of transition,  $-2\beta[\pi] \rightarrow 0\beta[n(\text{O})_z]$ , as in the vinylperoxy radical **1** itself. The absorption maximum of **8** is only slightly blue shifted compared with **1**.

The absorption maxima of radicals **1–7** were calculated for two extreme conditions, as  $Z$  and  $E$  conformers. In general, the  $E$  conformer is at lower energy. Usually, the energy difference is small, and both conformers including all intermediate conformers will contribute to the observed absorption. When the  $Z$  conformer is at relatively high energy ( $\Delta E > 10 \text{ kJ mol}^{-1}$ ),  $E$  conformers and conformers with high  $E$  character will predominate and determine the absorption spectrum.

The transitions of the phenylperoxy radical **9** orbitals [Fig. 4(a)] follow the same principle as those of the vinylperoxy radical **1**, but there are now two close-lying  $\pi$  orbitals. This results in two transitions,  $-2\beta[\pi] \rightarrow 0\beta[n(\text{O})_z]$  and  $-1\beta[\pi] \rightarrow 0\beta[n(\text{O})_z]$ , which together give rise to the long-wavelength absorption. Their average has to be taken, when the calculated value is compared with the experimental value.

The transitions of radicals **1–9** have considerable charge-transfer character, and for this reason the absorption maxima are red shifted with increasing dielectric constant of the medium. This is exemplified for the vinylperoxy **1** and phenylperoxy **9** radicals (Table 1). According to these data, the major changes in the red shift occur in the range from vacuum to moderate dielectric constants. For the phenylperoxy radical **9**, a red shift of about 10 nm is

**Table 3.** Calculation of the absorption maxima (oscillator strengths in parentheses) of the long-wavelength band of some peroxy and related radicals using the UTD/B3LYP/6–31G+(d,p) method *in vacuo* and in water (SCRF = PCM)<sup>a</sup>

Radical	Conformer	$\Delta E$ (kJ mol <sup>-1</sup> )	$\lambda_{\text{calc}}$ (nm)		$\lambda_{\text{exp}}$ (nm)	Transition
			Vacuum	Water		
	<b>9a</b> planar	15.9	409 (0.022)	479 (0.063)	490 (Ref. 8)	$-2\beta[\pi] \rightarrow 0\beta[\text{n(O)}_z]$
			448 (0.062)	508 (0.062)		$-1\beta[\pi] \rightarrow 0\beta[\text{n(O)}_z]$
	<b>9a</b> perp. <sup>b</sup>		381 (0.002)	457 (0.003)		$-2\beta[\pi] \rightarrow 0\beta[\text{n(O)}_z]$
			426 (0.0003)	503 (0.001)		$-1\beta[\pi] \rightarrow 0\beta[\text{n(O)}_z]$
	<b>9b</b> planar		397 (0.012)	452 (0.029)	490 (Ref. 8)	$-2\beta[\pi] \rightarrow 0\beta[\text{n(O)}_z]$
			464 (0.073)	497 (0.101)		$-1\beta[\pi] \rightarrow 0\beta[\text{n(O)}_z]$
	<b>9c</b> planar		409 (0.019)	482 (0.036)	560 (Ref. 8)	$-2\beta[\pi] \rightarrow 0\beta[\text{n(O)}_z]$
			471 (0.078)	542 (0.111)		$-1\beta[\pi] \rightarrow 0\beta[\text{n(O)}_z]$
	<b>9d</b> planar		388 (0.004)	456 (0.005)	590–600 (Ref. 8)	$-2\beta[\pi] \rightarrow 0\beta[\text{n(O)}_z]$
			508 (0.114)	594 (0.178)		$-1\beta[\pi] \rightarrow 0\beta[\text{n(O)}_z]$
	<b>10</b> planar	1.6 (2.2)	555 (0.012)	615 (0.010)	460 <sup>c</sup> (Ref. 12)	$-2\beta[\pi] \rightarrow 0\beta[\text{n(O)}_z]$
			616 (0.014)	676 (0.024)		$-1\beta[\pi] \rightarrow 0\beta[\text{n(O)}_z]$
	<b>10</b> perp.		526 (0.005)	568 (0.003)		
			588 (0.0001)	572 (0.007)		
	<b>11</b> planar	4.4 (1.8)	556 (0.003)	634 (0.005)	490 <sup>c</sup> (Ref. 12)	$-2\beta[\pi] \rightarrow 0\beta[\text{n(O)}_z]$
			625 (0.002)	721 (0.005)		$-1\beta[\pi] \rightarrow 0\beta[\text{n(O)}_z]$
	<b>11</b> perp.		489 (0.006)	585 (0.007)		
			505 (0.043)	597 (0.056)		
	<b>12</b> planar		409 (0.015)	490 (0.051)	400 <sup>c</sup> (Ref. 29)	$-2\beta[\pi] \rightarrow 0\beta[\text{n(O)}_z]$
			421 (0.012)	513 (0.001)		
	<b>13</b> planar		299 (0.134)	301 (0.166)	320 <sup>d</sup>	$0\alpha[\pi] \rightarrow +2\alpha[\pi^*] +$ $-1\beta[\pi] \rightarrow 0\beta[\pi]$

<sup>a</sup> Transitions as defined in the text. The energy differences ( $\Delta E$ ) between conformers *in vacuo* and in water (in parentheses).<sup>b</sup> Transition state of C—O bond rotation.<sup>c</sup> In acetonitrile.<sup>d</sup> This work.

observed on going from methanol to water.<sup>5,8</sup> In the calculations, a red shift of 3 nm at least reflects the trend.

Considerable effects of substituents on the absorption maxima of the phenylperoxy radicals **9a–d** were observed. An electron-donating substituent in the *para* position causes a considerable red shift, and this is well reflected in the calculations (Table 3). The electron-withdrawing cyano substituent does not shift the absorption maximum noticeably. According to the calculations, this is due to two effects, a larger energy gap between the two transitions that make up the broad absorption band and the higher oscillator strength of one of these transitions. Marked differences in the oscillator strengths of the

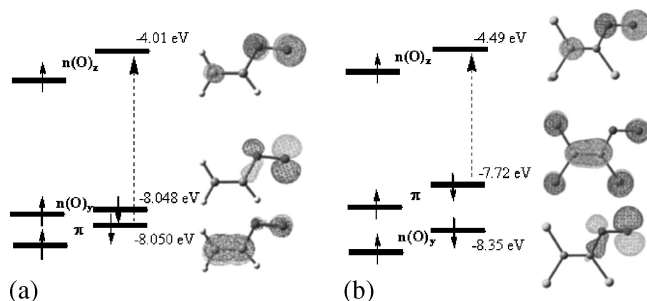
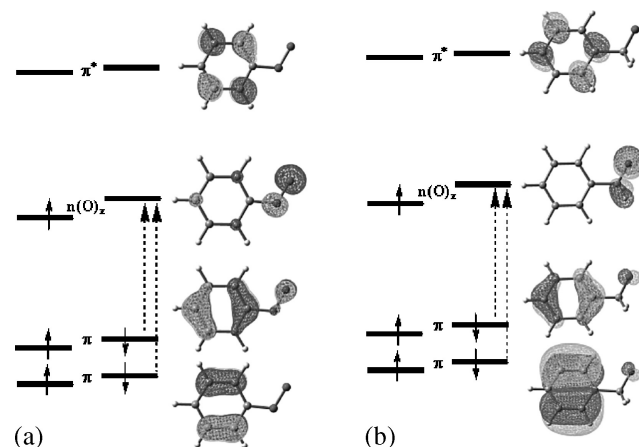
two relevant transitions are also observed with the electron-donating substituents —CH<sub>3</sub> and —OCH<sub>3</sub>, whereas for the unsubstituted phenylperoxy radical they are equal. In the calculations, the optimum configuration is planar. The perpendicular configuration is only a transition state between two equivalent planar conformations. Interestingly, when this configuration is calculated the oscillator strength is close to zero without a marked change in the absorption maximum.

The strong absorption band in the visible region of the benzoyloxy and cumyloxy radicals, **10** and **11**, is due to a  $-2\beta[\pi] \rightarrow 0\beta[n(\text{O})_z]$  plus  $-1\beta[\pi] \rightarrow 0\beta[n(\text{O})_z]$  transition, i.e. it is of the same type as the phenylperoxy



**Table 4.** Calculation of the absorption maxima (oscillator strengths in parentheses) of the long-wavelength band of some peroxy and related radicals using the UTD/B3LYP/6–31G+(d,p) method *in vacuo* and in water (SCRF = PCM)<sup>a</sup>

Radical	Conformer	$\lambda_{\text{calc}}$ (nm)		$\lambda_{\text{exp}}$ (nm)	Transition
		Vacuum	Water		
$\text{CH}_3\text{—S—O—O}\cdot$	<b>14</b>	458 (0.016)	487 (0.032)		$-1\beta[\text{n}(\text{S})_z] \rightarrow 0\beta[\text{n}(\text{O})_z]$
$\begin{array}{c} \text{OH} \\   \\ \text{S—O—O}\cdot \\   \\ \text{CH}_2\text{—CH}_2 \end{array}$	<b>15</b>	462 (0.013)	494 (0.032)	560 (Refs. 9–11)	$-1\beta[\text{n}(\text{S})_z] \rightarrow 0\beta[\text{n}(\text{O})_z]$
$\begin{array}{c} \text{O} \\    \\ \text{CH}_3\text{—C—O—O}\cdot \\    \\ \text{O} \end{array}$	<b>16</b>	272 (0.004) 297 (0.001)	272 (0.003) 294 (0.001)	Weak (Refs. 30, 31)	$-2\beta[\sigma] \rightarrow 0\beta[\text{n}(\text{O})_z]$ $-1\beta[\text{n}(\text{O})_x] \rightarrow +1\beta[\sigma^*]$
$\text{CH}_3\text{—O—O}\cdot$	<b>17</b>	239 (0.054)	248 (0.066)		$-2\beta[\text{n}(\text{O})_z] \rightarrow 0\beta[\text{n}(\text{O})_z]$
$\begin{array}{c} \text{CH}_3 \\   \\ \text{HO—C—CH}_2\text{—O—O}\cdot \\   \\ \text{CH}_3 \end{array}$	<b>18</b>	242 (0.036) 307 (0.002)	274 (0.010) 361 (0.002)	250 (Ref. 32)	$-3\beta[\text{n}(\text{OH})] \rightarrow 0\beta[\text{n}(\text{O})_z]$ $-2\beta[\sigma] \rightarrow 0\beta[\text{n}(\text{O})_z]$
$\begin{array}{c} \text{CH}_3 \\   \\ \text{HO—C—CH}_2\cdot \\   \\ \text{CH}_3 \end{array}$	<b>19</b>	255 (0.023)	242 (0.037)	225 (Ref. 32)	$0\alpha[\pi] \rightarrow +1\alpha[\sigma^*]$
$\begin{array}{c} \text{O} \\    \\ \text{CH}_3\text{—S}\cdot \\    \\ \text{O} \end{array}$	<b>20</b>	412 (0.006) 419 (0.024)	393 (0.007) 406 (0.032)	330 (Refs. 30, 31)	$-3\beta[\text{n}(\text{O})_z] \rightarrow 0\beta[\text{n}(\text{O})_z]$ $-1\beta[\text{n}(\text{O})] \rightarrow 0\beta[\text{n}(\text{O})_z]$
$\text{CH}_3\text{—S}\cdot$	<b>21</b>	328 (0.005)	333 (0.005)	Weak <sup>b</sup>	$-2\beta[\sigma] \rightarrow 0\beta[\text{n}(\text{S})_z]$

<sup>a</sup> Transitions as defined in the text.<sup>b</sup> Very weak, typically not detectable.**Figure 3.** MO schemes for transitions of the vinylperoxyl radical **1** (a) and the trichlorovinylperoxyl radical **7** (b) in water [UTD/B3LYP/6–31G+(d,p)/SCRF = PCM]**Figure 4.** MO schemes for the transitions of the phenylperoxyl radical **9** (a) and the benzoyloxyl radical **10** (b) in water [UTD/B3LYP/6–31G+(d,p)/SCRF = PCM]

radical **9**. For **10** and **11**, experimental data are only available for organic solvents, and for a comparison with the experiment calculations in the gas phase may possibly be more appropriate. Yet even then, agreement remains very poor when compared with the other radicals under investigation. The reason for this is not clear, but the fact that one may encounter such considerable deviations is a caveat for any assignments of intermediates merely on the basis of quantum-chemical calculations of their spectrum. It may be noted that for **10** there is a strong sensitivity of the calculated transition on the angle between the plane of the aromatic ring and the C—O bond. For example, in the case of the perpendicular conformation, changing the angle from optimized 100.7° to 96° leads to a 35 nm blue shift. The red shift on going from **10** to **11** is reflected in the calculations.

Interlacing a C=O group between the aromatic ring and the peroxy radical function as in **9/12** has a similar effect as in the vinyl analogues **1/8**.

The phenoxymethyl radical **13** is structurally related to **9** and **10**. However, only **9** and **10** show an absorption in the visible region, whereas **13** absorbs only in the UV region. This is due to a  $0\alpha[\pi] \rightarrow +2\alpha[\pi^*]$  plus  $-1\beta[\pi] \rightarrow 0\beta[\pi]$  transition, i.e. the  $\pi$ -system is also involved in this transition [Fig. 5(a)]. This is the reason why **13** absorbs much more towards the red than aliphatic alkoxyalkyl radicals that have absorption maxima <220 nm.<sup>28</sup> Radical **13** has practically no charge-transfer character, hence its absorption is not red shifted when the dielectric constant of the medium is increased.

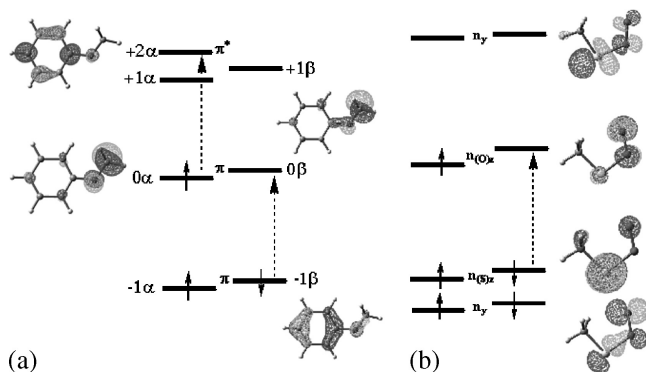


**Figure 5.** MO schemes for the transitions of the phenoxymethyl radical **13** (a) and the methylthiylperoxyl radical **14** (b) in water [UTD/B3LYP/6–31G+(d,p)/SCRF = PCM]

In the case of the alkylthiylperoxyl radicals **14** and **15** (experimental data are only available for **15**), the transition is from the n orbital at sulfur to the peroxy oxygen,  $-1\beta[n(S_z)] \rightarrow 0\beta[n(O_z)]$  [Fig. 5(b)]. The absorption,

located only in the UV region ( $<260\text{ nm}$ ),<sup>30,31</sup> of the sulfuranylperoxyl radical **16** has been assigned to a  $-2\beta[\sigma] \rightarrow 0\beta[n(O_z)]$  transition.

Alkylperoxyl radicals such as **17** and **18** typically absorb at longer wavelengths compared with their precursors, the alkyl radicals such as **19**. The latter absorb far in the UV region, and the transition has been assigned to a  $0\alpha[\pi] \rightarrow +1\alpha[\sigma^*]$  transition. Interestingly, in the case of the corresponding peroxyl radicals, functional groups may be involved in the transitions. Whereas the absorption of the methylperoxyl radical **17** has been assigned to a  $-2\beta[n(O_z)] \rightarrow 0\beta[n(O_z)]$  transition, the absorption of **18** is due to a  $-3\beta[n(OH)] \rightarrow 0\beta[n(O_z)]$  transition, that is, the OH group is involved in a kind of charge transfer. This being not very effective, the absorption remains in the UV region.

For reasons discussed below, sulfuranyl **20** and thiyl **21** radicals attracted our attention, and we therefore also report the transitions of their longest absorption band.

**Table 5.** Calculated [B3LYP/6–31+G(d,p)] reaction enthalpies for the formation of some peroxyl radicals [values in water (SCRF = PCM) in parentheses]

Radical	$\Delta H$ (kJ mol <sup>-1</sup> )	Experimental observation
	-197 (-207)	Irreversible O <sub>2</sub> addition to parent radical
	-145	Irreversible O <sub>2</sub> addition to parent radical
	-73	Irreversible O <sub>2</sub> addition to parent radical
	-66	Irreversible O <sub>2</sub> addition to parent radical
	-48	Reversible O <sub>2</sub> addition to parent radical
	-29/-46	Reversible O <sub>2</sub> addition to parent radical
	-31/-18/-17	Slow and reversible O <sub>2</sub> addition to parent radical
	-29 (-30)	Reversible O <sub>2</sub> addition to parent radical
	-9 (-3)	Reversible O <sub>2</sub> addition to parent radical
	+20/+31	No O <sub>2</sub> addition to parent radical

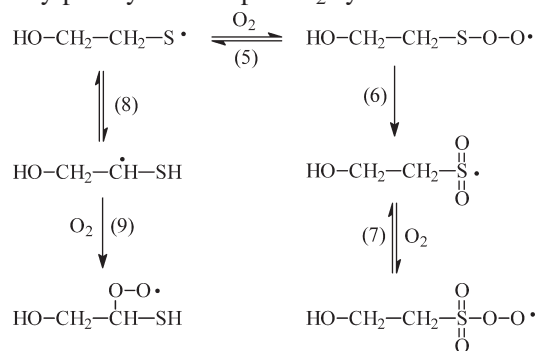
The transition of **20** is denoted  $-1\beta[n(O)] \rightarrow 0\beta[n(O)_z]$ . Thiyl radicals such as **21** are usually difficult to detect in laser flash photolysis or pulse radiolysis experiments. The reason for this is the low oscillator strength of the  $-2\beta[\sigma] \rightarrow 0\beta[n(S)_z]$  transition, where the  $\sigma$  orbital is orthogonal to the  $n$  orbital.

### Stability of peroxy radicals

Usually, the reaction of a carbon-centered radical with  $O_2$  is practically irreversible in aqueous solutions at room temperature. This also holds for the highly stabilized<sup>33–35</sup> peptide radicals.<sup>36</sup> However, there are exceptions, notably the alkylthiylperoxy radical<sup>9–11</sup> that we are interested in here and pentadienyl-type peroxy radicals. For example, the hydroxycyclohexadienyl radical (formed upon  $\cdot OH$  attack on benzene) undergoes reversible dioxygen addition both in aqueous solution<sup>37–39</sup> and in the gas phase.<sup>40</sup> Electron-withdrawing substituents retard the rate of  $O_2$  addition, and with the  $\cdot OH$  adducts to nitrobenzene, for example, this reaction is very slow.<sup>41</sup> Moreover, the phenoxyl radical does not react with  $O_2$  despite the fact that it has considerable spin density at carbon.<sup>42</sup> Table 5 gives the bond dissociation enthalpies (*BDE*) of various peroxy radicals calculated *in vacuo* and to account for potential solvent effects, for some of them also in aqueous solution.

### Around the chemistry of the alkylthiylperoxy radical

The reversibility of  $O_2$  addition to the alkylthiylperoxy radical [reaction (5)] is not the only complexity of the alkylthiylperoxy radical plus  $O_2$  system.



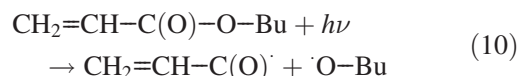
The latter can rearrange into the alkylsulfonyl radical which is more stable by  $160 \text{ kJ mol}^{-1}$  [reaction (6)]. In the presence of  $O_2$ , the alkylsulfonyl radical is converted into the corresponding peroxy radical [reaction (7)], a reaction that is also reversible.<sup>30,31</sup> The data in Table 5 indeed indicate a low *BDE*. From kinetic and product studies, it had been concluded that the alkylthiyl radical is also in equilibrium with the carbon-centered radical formed upon a 1,2-H shift [reaction (8)], but equilibrium (8) must be largely on the side of the thiyl radical. We have now calculated the energy difference between these

two radicals to be  $50 \text{ kJ mol}^{-1}$ . This value, considered accurate to no better than  $\pm 10 \text{ kJ mol}^{-1}$ , is fairly large, and evidently the thiyl radical must be the favoured species. However, any small equilibrium concentration of the carbon-centered radical will be scavenged irreversibly by  $O_2$  [reaction (9)], and this allows the reaction to proceed in this direction.

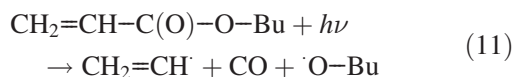
A quantum-chemical study on the alkylthiyl radical plus  $O_2$  system has already been carried out some time ago,<sup>14</sup> but the level of theory at that time was insufficient to calculate the UV-Vis spectra and the energetics of the various reactions properly. In fact, the assignment of the 560 nm absorption to the  $RSO_2\cdot$  species was challenged on the basis of these calculations.

### Photolysis of *n*-butyl acrylate

In the photolysis of *n*-butyl acrylate at 222 nm in solution, a major process is the scission of ester linkage ( $\alpha$ -cleavage):<sup>27</sup>



In a laser flash experiment in the presence  $O_2$ , a species grows in that absorbs near 430 nm. In principle, a double fragmentation could have occurred, i.e. CO and a vinyl radical may have been formed [reaction (11)], and this was confirmed by the observation of ethene and CO among the products.



For an assignment as vinylperoxy radical **1**, the observed absorption was somewhat blue shifted compared with that of authentic vinylperoxy radical. We therefore calculated the absorption maximum of the vinylcarbonylperoxy radical **8**. It turns out that it also has an absorption maximum in the visible region but at somewhat shorter wavelength than that of **1** (Table 3).

### CONCLUSION

The programs that are available to calculate the absorption spectra of free radicals are now fairly well advanced so that such calculations can be used to predict the positions of the absorption maxima. With radicals whose transitions have charge-transfer character, the dielectric constant of the medium has to be taken into account. However, a non-negligible error still persists (note the marked deviations between experiment and calculations in the case of the benzyloxyl-type radicals). Nevertheless, as shown for the radicals formed in the photolysis of *n*-butyl acrylate, under certain circumstances the



calculations can be extremely helpful, relatively easy to carry out and may be now routinely used to assist assignments in laser flash and pulse radiolysis studies.

## REFERENCES

1. von Sonntag C, Schuchmann H-P. *Angew. Chem. Int. Ed. Engl.* 1991; **30**: 1229–1253.
2. von Sonntag C, Schuchmann H-P. In *Peroxy Radicals*, Alfassi ZB (ed). Wiley: Chichester, 1997; 173–234.
3. Mertens R, von Sonntag C. *Angew. Chem. Int. Ed. Engl.* 1994; **33**: 1262–1264.
4. Alfassi ZB, Marguet S, Neta P. *J. Phys. Chem.* 1994; **98**: 8019–8023.
5. Alfassi ZB, Khaikin GI, Neta P. *J. Phys. Chem.* 1995; **99**: 265–268.
6. Alfassi ZB, Khaikin GI, Neta P. *J. Phys. Chem.* 1995; **99**: 4544–4548.
7. Khaikin GI, Neta P. *J. Phys. Chem.* 1995; **99**: 4549–4553.
8. Fang X, Mertens R, von Sonntag C. *J. Chem. Soc. Perkin Trans. 2* 1995; **2**: 1033–1036.
9. Jayson GG, Stirling DA, Swallow AJ. *Int. J. Radiat. Biol.* 1971; **19**: 143–156.
10. Tamba M, Simone G, Quintiliani M. *Int. J. Radiat. Biol.* 1986; **50**: 595–600.
11. Zhang X, Zhang N, Schuchmann H-P, von Sonntag C. *J. Phys. Chem.* 1994; **98**: 6541–6547.
12. Avila DV, Luszyk J, Ingold KU. *J. Am. Chem. Soc.* 1992; **114**: 6576–6577.
13. Avila DV, Ingold KU, Di Nardo AA, Zerbetto F, Zgierski MZ, Luszyk J. *J. Am. Chem. Soc.* 1995; **117**: 2711–2718.
14. Chatgililoglu C, Guerra M. In *Sulfur-Centered Reactive Intermediates in Chemistry and Biology*, Chatgililoglu C, Asmus K-D (eds). Plenum Press: New York, 1990; 31–36.
15. Krauss M, Osman R. *J. Phys. Chem.* 1995; **99**: 11387–11391.
16. Frisch MJ, Trucks GW, Schlegel HB, Scuseria GE, Robb MA, Cheeseman JR, Zakrzewski VG, Montgomery JA Jr, Stratmann RE, Burant JC, Dapprich S, Millam JM, Daniels AD, Kudin KN, Strain MC, Farkas O, Tomasi J, Barone V, Cossi M, Cammi R, Mennucci B, Pomelli C, Adamo C, Clifford S, Ochterski J, Petersson GA, Ayala PY, Cui Q, Morokuma K, Salvador P, Dannenberg JJ, Malick DK, Rabuck AD, Raghavachari K, Foresman JB, Cioslowski J, Ortiz JV, Baboul AG, Stefanov BB, Liu G, Liashenko A, Piskorz P, Komaromi I, Gomperts R, Martin RL, Fox DJ, Keith T, Al-Laham MA, Peng CY, Nanayakkara A, Challacombe M, Gill PMW, Johnson B, Chen W, Wong MW, Andres JL, Gonzalez C, Head-Gordon M, Replogle ES, Pople JA. *Gaussian 03, Revision B.02*. Gaussian: Pittsburgh, PA, 2003.
17. Becke AD. *J. Chem. Phys.* 1993; **98**: 5648–5662.
18. Becke AD. *J. Chem. Phys.* 1996; **104**: 1040–1046.
19. Lee C, Yang W, Parr RG. *Phys. Rev. B* 1987; **37**: 785–789.
20. *GaussView 2.1*. Gaussian: Pittsburgh, PA, 2000.
21. Barone V, Cossi M. *J. Phys. Chem. A* 1998; **102**: 1995–2001.
22. Klamt A, Schüürmann G. *J. Chem. Soc. Perkin Trans. 2* 1993; 799–805.
23. Rega N, Cossi M, Barone V. *J. Chem. Phys.* 1996; **105**: 11060–11067.
24. Barone V, Cossi M, Tomasi J. *J. Comput. Chem.* 1998; **18**: 404–417.
25. Bauernschmitt R, Ahlrichs R. *Chem. Phys. Lett.* 1996; **256**: 454–464.
26. Buxton GV, Stuart CR. *J. Chem. Soc. Faraday Trans.* 1995; **91**: 279–281.
27. Knolle W, Naumov S, Madani M, von Sonntag C. *Nucl. Instrum. Methods Phys. Res. B* 2005; in press.
28. Habersbergerova A, Janovsky I, Kourim P. *Radiat. Res. Rev.* 1972; **4**: 123–231.
29. Knolle W, Müller U, Mehnert R. *Phys. Chem. Chem. Phys.* 2000; **2**: 1425–1430.
30. Flyunt R, Makogon O, Schuchmann MN, Asmus K-D, von Sonntag C. *J. Chem. Soc. Perkin Trans. 2* 2001; 787–792.
31. Sehested K, Holcman J. *Radiat. Phys. Chem.* 1996; **47**: 357–360.
32. Simic M, Neta P, Hayon E. *J. Phys. Chem.* 1969; **73**: 3794–3795.
33. Viehe HG, Janousek Z, Mereny R, Stella L. *Acc. Chem. Res.* 1985; **18**: 148–154.
34. Reid DL, Armstrong DA, Rauk A, von Sonntag C. *Phys. Chem. Chem. Phys.* 2003; **5**: 3994–3999.
35. Reid DL, Armstrong DA, Rauk A, Nese C, Schuchmann MN, Westhoff U, von Sonntag C. *Phys. Chem. Chem. Phys.* 2003; **5**: 3278–3288.
36. Mieden OJ, Schuchmann MN, von Sonntag C. *J. Phys. Chem.* 1993; **97**: 3783–3790.
37. Pan XM, von Sonntag C. *Z. Naturforsch., Teil B* 1990; **45**: 1337–1340.
38. Pan X-M, Schuchmann MN, von Sonntag C. *J. Chem. Soc. Perkin Trans. 2* 1993; 289–297.
39. Fang X, Pan X, Rahmann A, Schuchmann H-P, von Sonntag C. *Chem. Eur. J.* 1995; **1**: 423–429.
40. Bohn B, Zetzsch C. *Phys. Chem. Chem. Phys.* 1999; **1**: 5097–5107.
41. Asmus K-D, Cercek B, Ebert M, Henglein A, Wigger A. *Trans. Faraday Soc.* 1967; **63**: 2435–2441.
42. Jin F, Leitich J, von Sonntag C. *J. Chem. Soc. Perkin Trans. 2* 1993; 1583.